

See discussions, stats, and author profiles for this publication at: <https://www.researchgate.net/publication/220012485>

Mass spectrometry/mass spectrometry by time-resolved magnetic dispersion

ARTICLE *in* ANALYTICAL CHEMISTRY · JULY 1983

Impact Factor: 5.64 · DOI: 10.1021/ac00259a032

CITATIONS

32

READS

11

3 AUTHORS:



[John T Stults](#)

Genentech

75 PUBLICATIONS 4,915 CITATIONS

SEE PROFILE



[Chris Enke](#)

University of New Mexico

198 PUBLICATIONS 4,554 CITATIONS

SEE PROFILE



[John F Holland](#)

Michigan State University

49 PUBLICATIONS 986 CITATIONS

SEE PROFILE

- (10) Williams, D. H.; Bradley, C.; Bojesen, G.; Santikarn, S.; Taylor, L. C. E. *J. Am. Chem. Soc.* **1981**, *103*, 5700-5704.
- (11) Barber, M.; Bordoli, R. S.; Sedgwick, R. D.; Tyler, A. N. *Biomed. Mass Spectrom.* **1982**, *9*, 208-214.
- (12) Standing, K. G.; Chait, B. T.; Ens, W.; McIntosh, G.; Beavis, R. *Nucl. Instrum. Methods* **1982**, *198*, 33-38.
- (13) Aberth, W.; Straub, K. M.; Burlingame, A. L. *Anal. Chem.* **1982**, *54*, 2029-2034.
- (14) Rudat, M. A.; McEwen, C. N. *Int. J. Mass Spectrom. Ion Phys.* **1983**, *46*, 351-354.
- (15) Hunt, D. F.; Bone, W. M.; Shabanowitz, J.; Rhodes, J.; Ballard, J. M. *Anal. Chem.* **1981**, *53*, 1704-1706.
- (16) Martin, S. A.; Costello, C. E.; Biemann, K. *Anal. Chem.* **1982**, *54*, 2362-2368.
- (17) Morris, H. R.; Panico, M.; Haskine, N. J. *Int. J. Mass Spectrom. Ion Phys.* **1983**, *46*, 363-366.
- (18) Ens, W.; Standing, K. C.; Westmore, J. B.; Oglvie, K. K.; Nemer, M. J. *Anal. Chem.* **1982**, *54*, 960-966.
- (19) Dell, A.; Morris, H. R. *Biochem. Biophys. Res. Commun.* **1982**, *106*, 1456-1462.
- (20) Stoll, R.; Schade, U.; Röllgen, F. W.; Giessmann, U.; Barofsky, D. F. *Int. J. Mass Spectrom. Ion Phys.* **1982**, *43*, 227-229.
- (21) Wong, S. S.; Stoll, R.; Röllgen, F. W. *Z. Naturforsch.*, A **1982**, *37A*, 718-719.
- (22) Röllgen, F. W., Institut für Physikalische Chemie der Universität Bonn, personal communication, 1982.
- (23) Taylor, G. I. *Proc. R. Soc. London, Ser. A* **1964**, *280*, 383-397.
- (24) Mahoney, J. F.; Yahiku, A. Y.; Daley, H. L.; Moore, R. D.; Perel, J. J. *Appl. Phys.* **1969**, *40*, 5101-5106.
- (25) Clappitt, R.; Altken, K. L.; Jefferies, D. K. *J. Vac. Sci. Technol.* **1975**, *12*, 1208.
- (26) Krohn, V. E.; Ringo, G. R. *Appl. Phys. Lett.* **1975**, *27*, 479-481.
- (27) Clappitt, R.; Jefferies, D. K. *Nucl. Instrum. Methods* **1978**, *149*, 739-742.
- (28) Seliger, R. L.; Ward, J. W.; Wang, V.; Kubena, R. L. *Appl. Phys. Lett.* **1979**, *34*, 310-312.
- (29) Ishitani, T.; Tamura, H.; Todokoro, H. *J. Vac. Sci. Technol.* **1982**, *20*, 80-83.
- (30) Day, R. J.; Unger, S. E.; Cooks, R. G. *Anal. Chem.* **1980**, *52*, 557A-572A.
- (31) Sakurai, T.; Culbertson, R. J.; Robertson, G. H. *Appl. Phys. Lett.* **1979**, *34*, 11-13.
- (32) Sudraud, P.; Colliex, C.; van de Walle, J. J. *Phys. (Orsay, Fr.)* **1979**, *40*, L207-L211.
- (33) Mair, G. L. R.; von Engel, A. J. *Appl. Phys.* **1979**, *50*, 5592-5595.
- (34) Swanson, L. W.; Schwind, G. A.; Bell, A. E.; Brady, J. E. *J. Vac. Sci. Technol.* **1979**, *16*, 1864-1867.
- (35) Culbertson, R. J.; Robertson, G. H.; Sakurai, T. *J. Vac. Sci. Technol.* **1979**, *16*, 1868-1870.
- (36) Swanson, L. W.; Bell, A. E.; Schwind, G. A.; Orloff, J. "Proceedings", Symposium on Electron and Ion Beam Science and Technology, St. Louis, MO, May 1980; Electrochemical Society: New York, 1980; p 594.
- (37) Swanson, L. W.; Schwind, G. A.; Bell, A. E. *J. Appl. Phys.* **1980**, *51*, 3453-3455.
- (38) Gamo, K.; Ukegawa, T.; Namba, S. *Jpn. J. Appl. Phys.* **1980**, *19*, L379-L382.
- (39) Gamo, K.; Ukegawa, T.; Inomoto, Y.; Ka, K. K.; Namba, S. *Jpn. J. Appl. Phys.* **1980**, *19*, L595-L598.
- (40) Dixon, A.; Colliex, C.; Sudraud, P.; van de Walle, J. *Surf. Sci.* **1981**, *108*, L424-L428.
- (41) Bell, A. E.; Schwind, G. A.; Swanson, L. W. *J. Appl. Phys.* **1982**, *53*, 4602-4605.
- (42) Mair, G. L. R.; von Engel, A. J. *Phys. D* **1981**, *14*, 1721-1727.
- (43) Thompson, S. P.; von Engel, A. J. *Phys. D* **1982**, *15*, 925-931.
- (44) Barofsky, D. F.; Giessmann, U.; Swanson, L. W.; Bell, A. E. "Proceedings", 29th International Field Emission Symposium, Göteborg, Sweden, Aug 1982; Andrén, H.-O., Nordén, H., Eds.; Almqvist and Wiksell Int.: Stockholm, 1982; pp 425-432.
- (45) Barofsky, D. F.; Giessmann, U.; Swanson, L. W.; Bell, A. E. *Int. J. Mass Spectrom. Ion Phys.* **1983**, *46*, 495-497.
- (46) Wagner, A.; Hall, T. M. *J. Vac. Sci. Technol.* **1979**, *16*, 1871-1874.
- (47) Magee, W. C. "Abstracts", 30th Annual Conference on Mass Spectrometry and Allied Topics, Honolulu, HI, June 1982; American Society for Mass Spectrometry: 1982, p 577.
- (48) Field, F. H. Presented in part at the 2nd International Meeting on Ion Formation from Organic Solids (IFOS II), Münster, FRG, Sept 1982.
- (49) Sigmund, P. In "Inelastic Ion-Surface Collisions"; Tolk, N. H., Tully, J. C., Helland, W., White, C. W., Eds.; Academic Press: New York, 1977; pp 121-152.

RECEIVED for review December 9, 1982. Accepted March 3, 1983. This work was supported by grants from the National Institutes of Health (AM 20937) and the National Science Foundation (ECS-8206796). Preliminary aspects of this study were presented at The 29th International Field Emission Symposium, Göteborg, Sweden, Aug 9-13, 1982, and the 9th International Mass Spectrometry Conference, Vienna, Austria, Aug 30-Sept 3, 1982.

Mass Spectrometry/Mass Spectrometry by Time-Resolved Magnetic Dispersion

John T. Stults and Christie G. Enke*

Department of Chemistry, Michigan State University, East Lansing, Michigan 48824

John F. Holland

Department of Biochemistry, Michigan State University, East Lansing, Michigan 48824

A new type of multidimensional mass spectrometer is presented. Utilization of ion beam pulsing and time-resolved detection techniques in a magnetic sector mass spectrometer allows simultaneous momentum and velocity analysis of the ions. This combination provides energy-independent ion mass assignments. Parent, daughter, and neutral loss spectra can be obtained as in conventional MS/MS instruments. Equations for mass determination are given and various scanning modes are described. Metastable ion decompositions are used to experimentally confirm the theory, and a comparison is made of the achieved and expected resolution and sensitivity. The potential for the technique in analytical applications is considered, particularly in light of a proposed high-speed data acquisition system.

The ability to identify relationships between parent and daughter ions that result from metastable ion decomposition

or from collision-induced dissociation (CID) has become increasingly important in recent years. Spectra showing all the daughters of a specific parent ion (daughter spectra) are proving invaluable for many applications in mixture analysis and structure elucidation (1-3). So also are spectra which show all the parents of a particular daughter mass (parent spectra) or spectra of ions that undergo a particular neutral loss (neutral loss spectra). These types of spectra are normally obtained by a technique referred to as mass spectrometry/mass spectrometry (MS/MS), that utilizes various tandem (sequential) arrangements of mass-selective devices.

Two types of MS/MS instruments are commonly in use and are commercially available: tandem sector instruments of which the mass-analyzed ion kinetic energy spectrometer (MIKES) (4) is an example, and multiple quadrupole instruments such as the triple quadrupole mass spectrometer (TQMS) (5). Both types of instruments operate in a sequential manner: (a) ion formation (b) parent ion selection, (c) parent ion dissociation, (d) daughter ion selection, and (e) ion de-

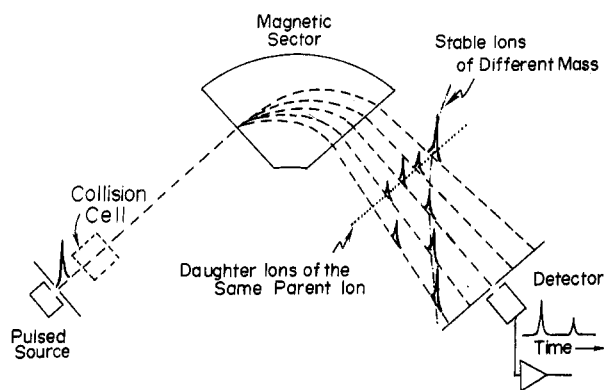


Figure 1. Ion separation by momentum and velocity in a time-resolved magnetic dispersion mass spectrometer. Daughter ions from the same parent mass appear at the same arrival time but are dispersed according to their momenta. Stable ions have shorter arrival times than daughter ions of the same momentum because of their greater initial velocity.

tection. The sequential nature of the mass selection operations, however, allows examination of only one combination of parent and daughter ion masses at a time. Many analyses require the identification of only a specific compound or class of compounds for which measurement of relatively few parent and daughter ions will suffice. Molecular identification or structure elucidation of unknown compounds can necessitate the collection of the complete MS/MS data field (all the daughters of all the parents). This process can require tens of seconds to several minutes. Thus full MS/MS analysis is available only for samples that can be continuously introduced into the ion source over a relatively long time.

A potentially much faster method for generation of the multidimensional MS/MS data is through simultaneous momentum and velocity measurements. Such measurements can be made with a single sector mass spectrometer modified for ion source pulsing and time-resolved detection. The magnetic sector provides analysis of ion momentum while the combination of a pulsed ion source and time-resolved detection system provides analysis of the ion velocity through the instrument. In this configuration there is not a separate time-of-flight section, but rather the flight time is measured *through* the magnetic sector instrument. Since the ion optics rigidly define the radius of curvature at which ions are detected, the distance traveled by all observed ions will be the same.

Figure 1 illustrates the basic components of a single sector mass spectrometer and shows the separation of ions based on velocity and momentum. Approximately monoenergetic ions extracted in a brief pulse from the source may undergo fragmentation in the field-free region preceding the magnet. The magnetic field disperses the ions according to their momenta, daughter ions now having less momentum than their parents. At the same time, ions become separated along the ion path as a result of their different velocities. Unlike the momentum, however, the velocity of a daughter ion remains essentially the same as that of its parent ion, altered only slightly by the dissociation process, so all daughter ions of the same parent will have nearly identical velocities. For a single value of the magnetic field, the ion packet corresponding to stable ions with the selected momentum will arrive at the detector, followed in time by daughter ions with the same momentum which originated from fragmentations of progressively heavier (and slower) parents. If a current-time curve is taken for each value of magnetic field strength (momentum), the complete set of MS/MS spectra for the sample can be obtained from the resulting data set. As will be shown, the mass assignment for any ion (daughter or stable

ion) is based solely on the combination of its field strength and arrival time and is completely independent of its energy. Daughter ion, parent ion, and neutral loss spectra can be constructed from the complete data set or can be obtained by various independent and linked scans of the magnetic field strength and ion arrival time.

Time-resolved detection of magnetically dispersed ions can be accomplished with instrumentation that is simpler and more commonly available than tandem MS/MS instrumentation and could provide the complete MS/MS data field at a dramatically greater rate. The theory of operation of this new type of mass spectrometer is developed in this paper, and data from the first experimental implementation are compared with this theory.

THEORY

Mass Assignment for Parents and Daughters. For a mass spectrometer in which the ions are accelerated out of the source with the same kinetic energy, the velocity of the ions is given by eq 1, where m is the ion mass, v is the velocity,

$$\frac{1}{2}mv^2 = zeV \quad (1)$$

z is the number of charges on the ion, e is the electronic charge, and V is the accelerating voltage. Either by pulsing the accelerating voltage or deflecting the ion beam, a pulse of nearly monoenergetic ions can be produced (assuming $z = 1$). After acceleration, the velocity of any ion is inversely proportional to the square root of its mass. As the accelerated ions travel through space, they separate according to mass, the lightest ions traveling fastest. The time-of-flight, t , of ions reaching a detector of fixed distance, l , from the pulsing device is given by eq 2. Equations 1 and 2 can be combined to give eq 3—an

$$t = l/v \quad (2)$$

expression relating the mass-to-charge ratio of an ion to its flight time. This is the equation for mass determination in a time-of-flight (TOF) mass spectrometer.

$$\frac{m}{z} = \frac{2Ve t^2}{l^2} \quad (3)$$

Ions traveling at right angles to a uniform magnetic field are dispersed along various arcs according to their momenta, as given by eq 4, where B is the magnetic field strength and

$$mv = Bzer \quad (4)$$

r is the radius of each ion's circular path. Simultaneous measurement of the flight time of an ion (inversely proportional to velocity) and the magnetic field at which that ion passes the detector entrance slit (proportional to momentum) provides the necessary data for determination of the ion mass. This is expressed in eq 5 which can be derived by combining eq 2 and 4. Thus, the combination of a momentum analyzer

$$\frac{m}{z} = Bt \left(\frac{er}{l} \right) \quad (5)$$

and a velocity analyzer effectively produces a mass-to-charge ratio determination that is independent of ion energy. An important consequence of this energy-independent mass determination is the ability to accurately assign the mass, even for a single ion, and this relation holds for stable ions as well as ions which change mass in the field-free region between the ion acceleration region and the magnetic sector. This fact can be exploited to perform experiments normally done with a tandem mass spectrometer.

A daughter ion, arising from either unimolecular decay or collision-induced dissociation occurring in the field-free region preceding the magnet, will be transmitted to the detector when

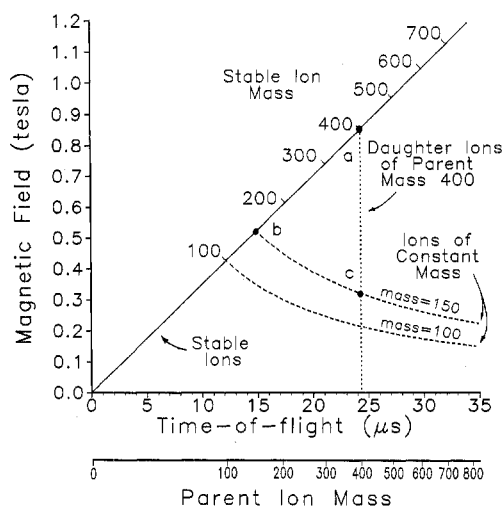


Figure 2. MS/MS data field (B vs. t). Each line represents the locus of peaks for different types of ions ($V = 3500$ V, $l = 1.0$ m, $r = 0.2$ m). All coordinates below the stable ion line represent daughter ions. The points show the location of peaks for (a) stable ions of mass 400, (b) stable ions of mass 150, and (c) daughter ions of mass 150 with parent of mass 400.

the field strength corresponds to its true momentum. The combination of magnetic field strength and arrival time can be used to make an accurate mass assignment according to eq 5. Thus masses of all stable and daughter ions will be determined accurately by the combination of momentum and velocity. The velocity of a daughter ion will be nearly the same as that of its precursor (parent) ion since the release of kinetic energy in the fragmentation process alters the velocity only slightly (6). Hence, the use of the measured flight time of the daughter ion can be used in eq 3 to identify the mass of the parent from which the daughter originated. The possible spread in daughter ion velocities through fragmentation might, however, make it more difficult to tell which of the stable ions in a closely packed cluster is the true parent. Thus, even though parent and daughter ion masses are determined accurately, in the MS/MS modes this technique is analogous to tandem MS/MS techniques in which the resolution of parent mass selection is poorer than that of the daughter analysis. In a later section, centroiding techniques are suggested which can improve the mass resolution of parent identification.

MS/MS Scans Available. With the ability to determine parent and daughter masses comes the need to combine them to obtain meaningful results. For instance, all daughter ions of a single parent ion provide a "mass spectrum" of the parent. The various MS/MS scans that have evolved can all be obtained with the time-resolved magnetic dispersion mass spectrometer and a scanning time-slice detector as used in current TOF mass spectrometers. Consider Figure 2, a computer-generated plot of magnetic field strength vs. ion flight time showing the expected loci of peaks for several types of scans, i.e., each line marks the possible values of B and t along which peaks might be observed for the indicated scan. If the arrival time slice that is sampled is held constant at the flight time of a parent ion, only a parent ion and its daughters will be detected when the magnetic field is scanned. The result is a daughter ion scan, which is shown for parent mass 400 u.

A parent ion scan produces a spectrum of all parents that undergo fragmentation to produce a particular daughter ion. This is achieved by scanning the sampled time slice along with the magnetic field strength so that the product Bt is kept constant. In this linked scan at constant Bt , ions of the same mass will be measured, the arrival times revealing the masses of the parents that produced the selected daughter mass.

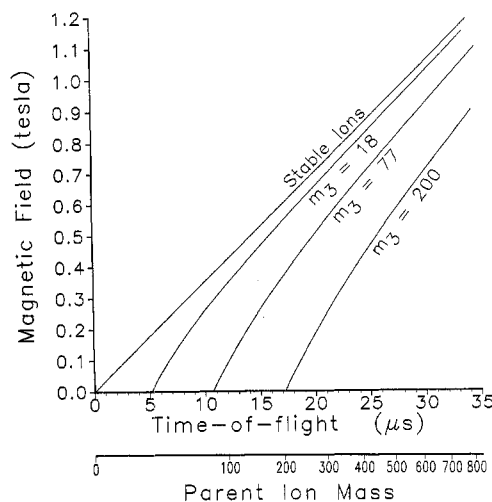


Figure 3. MS/MS data field showing the locus of peaks for stable ions and daughter ions resulting from several representative neutral losses, m_3 ($V = 3500$ V, $l = 1.0$ m, $r = 0.2$ m).

One additional type of scan, often useful for the screening of mixtures, is the neutral loss scan. This is a scan of all the parents that fragment to lose a particular neutral mass. The neutral mass that is lost in the fragmentation process $m_3 = m_1 - m_2$, can be held constant by a more complex linked scan, as given by eq 6, the difference of eq 3 and 5. A plot of B

$$m_3 = \frac{2Vet^2}{l^2} - \frac{Bret}{l} \quad (6)$$

vs. t illustrating this linked scan is shown in Figure 3. Analogous to Figure 2, this plot shows several lines, each marking all possible values of B and t for the stable ion or neutral loss scan indicated.

Mass assignment for an ion that does not decompose after leaving the source, i.e., a stable ion, should be the same whether calculated from eq 3 or eq 5. Equations 3 and 5 can be combined to give eq 7 which is only valid for stable ions.

$$t_s = Brl/2V \quad (7)$$

This equation indicates the flight time at which a stable ion can be observed for a given value of the magnetic field and is represented as the diagonal line in Figures 2 and 3. Thus, by limiting the observation to combinations of flight time and magnetic field strength which satisfy eq 7, stable ions can be determined while screening out any ions that result from metastable or CID fragmentation processes. Conversely, by summing all ions for which the arrival times are longer than t_s while scanning B , a spectrum of daughter ions without any stable ions would be obtained. Such a "metastable spectrum" might be useful as a fingerprint for a compound.

Each of the MS/MS scans discussed could be obtained individually, although sometimes necessitating complex linked scanning of the magnetic field and sampled arrival time. Similarly, each of the scans could be constructed from an array of intensities from all combinations of B and t if all the points were collected. The advantages of each approach will be discussed, especially the features of the time-resolved magnetic dispersion mass spectrometer that make array detection possible.

EXPERIMENTAL SECTION

Experiments were performed on an LKB-9000 mass spectrometer. The instrument was not altered physically and was operated in the normal manner with the exceptions noted below. The ion beam deflection plates, normally used for focusing and located immediately after the entrance slit, were used to rapidly move the ion beam up and down and thus produce a packet of

ions (7, 8). Each deflection plate was connected to a separate high voltage dc power supply. After the voltage on each plate was adjusted to give maximum ion beam focus, a 50-V peak-to-peak square wave signal was superimposed on the voltage of one of the plates to deflect the ion beam. The beam was deflected away from the exit slit during the HI and LO levels of the square wave so that only during a portion of the rising and falling edges of the square wave was the beam focused on the exit slit. The rising edge of the square wave signal was also used as a start time trigger for the time-resolved readout.

The output current of the electron multiplier was converted to a voltage and amplified with a wide band Comlinear Model CLC 103 DC amplifier (Comlinear Corp., Loveland, CO). An oscilloscope was used in focusing the ion beam and making resolution measurements. A PAR Model 162 boxcar averager (Princeton Applied Research, Princeton, NJ) with Model 164 gated integrator was used to make time-resolved measurements. Results were recorded on a strip chart recorder. Pressure in the ion source housing was maintained at 2×10^{-6} torr. The trap current was 120 μ A and the accelerating voltage was 3500 V. The electron multiplier voltage was -2.1 kV for stable ions and -3.1 kV for daughter ion detection.

To experimentally test the theory of the technique and evaluate the performance of the instrument, a single compound that exhibits a large number of metastable peaks, *n*-decane, was chosen. The *n*-decane was reagent grade and was introduced via the heated gas inlet. Over 100 metastable ion decompositions have been observed for *n*-decane (9, 10) but only a few were used in this experiment. Other peaks were doubtless present but due to the sensitivity limitations of the present implementation and the tedious method of acquiring data, only the most intense peaks were chosen for measurement. This implementation was selected for its ability to adequately demonstrate the principles of this new technique without the development of extensive new instrumentation. An automated instrument with improved efficiency is now under construction in our laboratory.

Magnetic Field and Time Measurements. The measurements were made by manually setting the magnetic field and then measuring the arrival time spectrum by scanning the gated integrator aperture delay. The magnetic field strength was taken from the digitized output of a Hall probe. Since the transfer function for the field detection components was not known precisely, the values measured were arbitrarily assigned as field strength units (fsu). The actual value of the field strength is $B = bC$ where b is the measured value in fsu and C is the unknown conversion factor with units of T fsu $^{-1}$. A calibrated mass marker was used to obtain stable ion masses. The stable ions of *n*-decane were thus used to calibrate the system, although any compound with known masses could have been used. Experimental values for the parent and daughter masses were calculated from eq 3 and 5.

RESULTS

When deriving the equations in the Theory section, we assumed that, among other things, the starting time of the ion source pulse is known accurately and that the ions experience no accelerating fields after leaving the ion source region. Initial data analysis and study of the ion flight path revealed that these assumptions were not valid in the present instrumental configuration. The difference in time between the readout start time trigger and the start of the ion pulse is reasonably constant, but not predictable. This leads to a constant offset in the measured arrival times. Secondly, the ions experience additional acceleration in a small region between the exit slit (at ground potential) and the electron multiplier (-1.5 kV to -3.5 kV depending on the gain setting). This acceleration is mass dependent and as a result daughter ions receive a larger velocity increase than their heavier parents. This effect is further enhanced by use of different electron multiplier gains for detection of stable and daughter ions. Corrections were made to eliminate the effect of these two factors before fitting the data to the equations.

To determine the time offset, t_{offset} , the stable ion data were plotted as t vs. m (see eq 3). Linear least-squares regression

Table I. Stable Ion Measurements

actual mass	$t_{\text{measd}}, \mu\text{s}$	$t_{\text{corr}}, \mu\text{s}$	$b_{\text{measd}}, \text{fsu}$	$b_{\text{corr}}, \text{fsu}$
39.0	9.08	7.58	21.19	21.33
41.0	9.28	7.78	21.70	21.84
42.0	9.34	7.84	21.95	22.09
43.0	9.44	7.94	22.23	22.37
56.1	10.59	9.07	25.36	25.50
57.1	10.67	9.15	25.57	25.71
70.1	11.66	10.13	28.37	28.51
71.1	11.74	10.21	28.57	28.71
84.1	12.66	11.12	31.06	31.20
85.1	12.72	11.18	31.26	31.40
99.1	13.64	12.09	33.75	33.89
113.1	14.46	12.90	36.08	36.22
142.2	16.01	14.43	40.48	40.62

^a fsu = field strength units, defined in the text.

gave a value for the intercept, $t_{\text{offset}} = 1.42 \pm 0.02 \mu\text{s}$. To correct for the additional acceleration region, the transit time from the exit slit to the electron multiplier, t_{EM} , was calculated for each ion and subtracted from the measured arrival time. The value of t_{EM} was determined from the distance between the exit slit and the electron multiplier, d , and from the average velocity of each ion in this region, assuming constant acceleration. The average velocity is calculated from the accelerating voltage, V_1 , and the electron multiplier voltage, V_2 , according to eq 8, where m_1 is the parent ion mass and m_2 is the daughter mass. For stable ions, $m_1 = m_2$. The distance traveled was estimated to be 1–2 cm. A value of 1.2 cm for the distance d gave the best results.

$$v' = \frac{1}{2} \left\{ \left[\frac{2eV_1}{m_1} \right]^{1/2} + \left[\frac{2e}{m_2} \left(\frac{m_2}{m_1} V_1 + V_2 \right) \right]^{1/2} \right\} \quad (8)$$

The corrected arrival times $t_{\text{corr}} = t_{\text{measd}} - t_{\text{offset}} - t_{\text{EM}}$ are listed in Table I for the stable ions and Table II for the daughter ions. The corrected times for the stable ions were fit to eq 3 to give the value of $2Ve_z/l^2 = 0.681 \pm 0.003 \text{ u } \mu\text{s}^{-2}$. This compares favorably with a value of $0.675 \text{ u } \mu\text{s}^{-2}$ calculated from $V = 3500\text{V}$, $l = 1.00 \text{ m}$.

Parent mass assignments for the daughter ions were calculated from eq 3 by using corrected flight times and the value of $2Ve_z/l^2$ obtained from the stable ion data. The mass assignments are listed in Table II. In the present instrumental configuration, approximate values for m_1 and m_2 must be found for the daughter ions before t_{EM} can be calculated. However, since t_{EM} is a small correction, relatively large errors in the approximation of m_1 and m_2 can be tolerated with little effect on the value of t_{corr} .

As in the case of arrival times, an offset in the magnetic field measurements was observed. To determine this offset a plot of b vs. m was made, according to eq 9. (Equation 9

$$\frac{m}{z} = \frac{B^2 r^2 e}{2V} = \frac{(bC)^2 r^2 e}{2V} \quad (9)$$

is commonly used to describe mass separation in magnetic sector mass spectrometers and is derived from equations 1 and 4.) Linear regression gave an intercept of $b_{\text{offset}} = -0.14 \pm 0.02 \text{ fsu}$.

The corrected values of b and t for the stable ions were fit to eq 5 to obtain a value of $er/l = 0.2423 \pm 0.0003 \text{ u } \mu\text{s}^{-1} \text{ fsu}^{-1}$. With this value for er/l , the daughter ion masses were calculated from corrected values of b and t . These mass assignments are given in Table II. The value of er/l was calculated a second time using daughter ion data and actual daughter masses. Comparison of the two values of er/l by the Student t test showed no difference. This provides additional verification of the theory by showing that eq 5 is

Table II. Daughter Ion Measurements and Mass Assignments

actual mass		$t_{\text{measd}}, \mu\text{s}$	$t_{\text{corr}}, \mu\text{s}$	$b_{\text{measd}},^a \text{fsu}$	$b_{\text{corr}}, \text{fsu}$	calcd mass		% rel intens
m_1	m_2					m_1	m_2	
41.0	39.0	9.26	7.76	20.62	20.76	41.0	39.0	0.2
43.0	41.0	9.40	7.90	21.21	21.35	42.5	40.9	0.3
57.1	41.0	10.64	9.13	18.44	18.58	56.8	41.1	0.6
70.1	55.0	11.66	10.14	22.29	22.43	70.0	55.1	0.2
71.1	43.0	11.70	10.18	17.32	17.46	70.6	43.1	0.8
84.1	69.1	12.62	11.09	25.51	25.65	83.8	68.9	0.2
85.1	43.0	12.66	11.14	15.84	15.98	84.5	43.1	0.4
85.1	57.1	12.70	11.17	20.95	21.09	85.0	57.1	0.5
99.1	57.1	13.54	12.06	19.44	19.58	99.0	57.2	1.2
113.1	57.1	14.40	12.86	18.22	18.36	112.6	57.2	0.3
113.1	71.1	14.42	12.88	22.67	22.81	113.0	71.2	0.6
142.2	85.1	15.98	14.42	24.17	24.31	141.6	84.9	0.1
142.2	99.1	15.96	14.40	28.14	28.28	141.3	98.7	0.3
142.2	113.1	16.02	14.46	32.19	32.33	142.4	113.3	0.4

^a fsu = field strength units, defined in the text.

equally valid for stable and daughter ions, as expected. Thus, by considering the flight path and timing inaccuracies, the experimental results fully support the theory.

The mass assignment accuracy is presently limited by the resolution and by the signal-to-noise ratio. Resolution can be evaluated in two ways, according to the precision of the magnetic field and flight time measurements and according to the peak widths observed. The time of flight could be measured reproducibly to within about 30 ns. However, peak widths were on the order of 200 ns (full width at half-height) corresponding to 10 u, making it difficult to ascertain the center of the peak, especially when the signal-to-noise level was low. The magnetic field could be measured reproducibly to 1 part in 10 000 but peak widths were on the order of 0.5 u.

The signal levels for the daughter ions were very low compared with the parents. Some averaging was performed but several of the daughter ions were measured with a signal-to-noise ratio of as low as 3. A higher gain electron multiplier, better signal amplification, additional signal averaging, and inclusion of a collision cell could improve the data significantly. Work is under way to make these improvements.

DISCUSSION

The data obtained from the current implementation of the technique and presented in the previous section verify that time-resolved magnetic dispersion mass spectrometry is feasible since daughter ions are clearly distinguished from parent ions and from each other, and the mass assignments and parent-daughter relationships follow those expected from the theory. However, the performance in mass resolution and sensitivity were severely limited by this implementation; no internal modifications of the ion optics were made for optimizing performance with pulsed operation. In this section, the basic factors affecting these characteristics are developed and the resulting limitations and capabilities of this new technique are explored.

Mass Assignment and Resolution for Stable Ions and Daughter Ions. A discussion of resolution can be divided into two parts, one concerning the precision of the measurement (the instrumental resolution), the other regarding the observed peak widths (the mass resolution). Both factors contribute to the mass assignment accuracy and precision, as will be seen. The factors contributing to the imprecision in the mass assignments of both parent and daughter ions are principally the precision in the measurements of flight time and magnetic field strength according to eq 5. The precision in the magnetic field measurement is determined by the field inhomogeneity, field stability, the effect of fringing fields, as well as the precision of the signal from the magnetic field

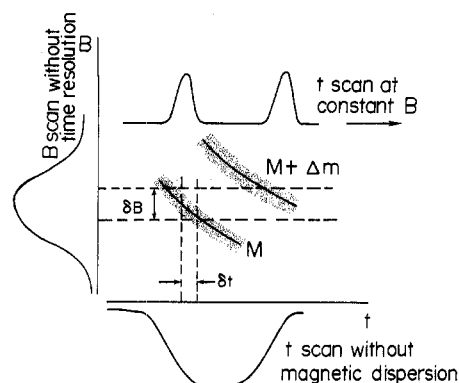


Figure 4. Expanded portion of B - t plane illustrating the resolution characteristics. Solid line represents ion intensity when the uncertainty in the radius and flight length is zero. Shaded portions represent the ion intensity for uncertainties in r and l . The uncertainties in the field strength and time define the region of the B - t plane sampled.

sensor, and the accuracy of any calibration procedure. The uncertainty in path radius is determined by the slit widths. The resulting mass uncertainty due to the magnetic sector should be the same as that obtained with the magnetic spectrometer operated in normal (non-time-resolved) mode with *monoenergetic ions*. Timing precision is limited by the uncertainty in the start time, the accuracy in measuring the delay time, and the aperture window of the sampling electronics. Precision in the flight length is determined by the depth of the ion volume sampled and by the different paths through the magnetic sector due to first-order focusing in the sector. Flight time precisions comparable to those obtained with conventional time-of-flight mass spectrometers when measuring monoenergetic ions with no metastable decompositions should be achievable (0.5–1.0 ppt).

The diagram of Figure 4 is an expanded portion of a hypothetical B - t plane for two stable ions differing by one mass unit. The solid curves represent the signal expected when the uncertainty in the radius and path length is zero. The shaded regions containing the solid curves represent the "width" of each curve determined by uncertainties in the radius and path length. The uncertainties in B and t are also shown. Energy differences in ions of the same mass will cause them to spread out along the lines of constant Bt as shown by the length of the line but will cause no increase in the width of the line. For a single mass, higher energy ions will appear at shorter arrival times and higher field strengths. This energy spread in ions of the same mass affects the separate resolutions of B and of t but not of Bt . Thus, resolution in two dimensions and the use of the Bt product for mass assignment remove

the effect of energy spread as a limiting factor in mass determination. Hence, the time-resolved magnetic dispersion mass spectrometer should provide unit mass resolution to 1000 u for both stable and daughter ion masses. Conversely, measurement of the distribution of ions along the line of constant Bt will provide an energy spread profile useful for studying the energetics of ion formation or fragmentation (11).

The diagram of Figure 4 can also be used to compare the resolutions expected for simple magnetic, simple time-of-flight, and time-resolved magnetic dispersion mass spectrometers. In the magnetic instrument with no time resolution, the ion intensity would be projected onto the B axis only. The right end of the higher mass peak will overlap with the left end of the lower mass peak to give less than fully resolved peaks. Likewise, in a TOF instrument, the two peaks will overlap on the time axis giving less than complete resolution. On the other hand, the time-resolved mass spectrometer determines a two-dimensional section of the plot and as such is potentially capable of a higher resolving power than with either B or t separately. The masses represented by the two curves will be completely resolved if the region delineated by δB and δt contains relatively little ion intensity in the space between the adjacent Bt curves even if the masses are not resolved by B or t alone. As the mass increases, the resolution will decrease because of the decreasing separation of the Bt curves of adjacent mass values.

Energy focusing, normally required in time-of-flight analysis to improve the resolution (12, 13), is not needed. Space focusing to correct for variations in the point of ion formation in the source can be optimized without the need to worry about its incompatibility with energy focusing (14). One way to view this technique, at least for stable ion analysis, is that the magnet is acting as an energy filter for TOF analysis. Indeed, magnets have been previously used with TOF to filter out ions with large energy deviations, such as those produced in laser desorption (15, 16). Magnets have also been proposed for focusing ions with equal momentum acceleration (17). Thus, magnetic dispersion could provide an alternative to other methods of dealing with energy spreads, such as the Mamyrin reflectron (18).

Mass Assignment and Resolution for Parent Ion Determinations. Due to the release of kinetic energy during the dissociation process (typically less than 1 eV) the energy spread of the daughter ions will be greater than that for stable ions. In the previous section it was shown that this has no effect on the accuracy of daughter mass assignment because the value of Bt is not affected. The selection of the parent ion which gives rise to a given daughter is, however, based on the flight time of the daughter ion. Therefore, peak broadening along the time axis, especially for higher masses and for large kinetic energy releases, could make it difficult to assign a parent mass for a daughter ion if there are several possible parents within that same velocity range. Correct assignment of the parent ion mass in this case could be aided by peak intensity centroiding along the Bt curve for both parent and daughter ions. For more serious cases involving daughter ion arrival time overlap, deconvolution, factor analysis, or other chemometric techniques could be invoked.

Dissociations within Non-Field-Free Regions. An additional factor that will affect the appearance of the spectrum and the mass resolution is the dissociation of ions during acceleration or within the magnetic sector itself. Dissociations within the accelerating field do not affect the daughter ion mass assignment because this mass assignment is solely defined by the value of Bt . The arrival time will decrease, though, resulting in a low-level continuum along the curve of constant Bt between the arrival time for a stable ion and the arrival time for the same transition occurring in the field-free

region. Likewise, dissociations within the magnetic sector result in a continuum that extends from the stable ion Bt position to the daughter ion Bt position along a line of constant arrival time. The intensity along the continuum should be very small compared to the intensity at the Bt of the daughter ion because all dissociations occurring in the field-free region are concentrated there while all occurring in the magnet are distributed along the continuum. The use of a collision cell to enhance dissociations in the field-free region will further suppress the continuum intensity.

Sensitivity. The expected sensitivity of the time-resolved magnetic dispersion mass spectrometer can be estimated by comparison with a conventional magnetic sector mass spectrometer. Relative to the conventional instrument, sensitivity will be limited by the low duty cycle of the ion beam pulsing (the time the beam is "on" relative to the total period of the pulsing cycle) and the increased resolution in both time and magnetic field strength necessary when precise mass values are required. The loss of ion intensity due to pulsing depends on the mechanism used to create the pulse. Continuous ionization and ion extraction followed by beam deflection (7, 8) discards all ions which are not within the sampled segment of the ion beam. Signal strength in this case is attenuated by the value of the duty cycle. For example, if time resolution requirements necessitate approximately a 10 ns wide ion packet, with a cycle duration of 25 μ s, only 10 ns/25 μ s (0.0004) of the ions extracted would be utilized. In other words, this technique would provide a sensitivity of 0.0004 times that of the same magnetic instrument without velocity analysis. Fortunately, the beam deflection technique represents the worst case.

A more favorable source pulsing mechanism is the one used in conventional time-of-flight instruments. Ions are generated for a period of time between pulses after which a voltage pulse is applied to an extraction grid to form the ion packet. Some of the ions formed between pulses are held in the source by the space charge of the electron beam until the extraction takes place. For example, holding and extracting only 4% of the ions produced between pulses would result in 100 times more ion charge in the packet than the beam deflection technique would give. Other methods of efficient ion generation or ion storage prior to extraction may also prove useful. When pulsed desorption/ionization from a sample surface is used, for example, virtually no sample need be lost between pulses.

The addition of time resolution to the momentum resolution of the sector instrument can result in a loss in sensitivity of the same type that is observed when an electric sector is added to a magnetic sector to form a double-focusing instrument. As the previous discussion of resolution demonstrated, precision in the mass assignment is limited by the precision in the measurement of the arrival time. Obviously, decreasing the arrival time aperture would lead to a concomitant loss in sensitivity at any one time slice. As with other types of resolving instrumentation, sensitivity and resolution are reciprocally related and trade-offs are made based upon specific analysis requirements.

Time-Resolved Detection Techniques. In conventional time-of-flight mass spectrometry, recorded spectra, either on paper or in digital form, are normally obtained with a gated detection scheme in which ions of only one arrival time are detected in a narrow time slice or aperture that is triggered at a specified delay after the ion pulse is initiated. (This can be called time-slice detection of TSD). The aperture delay then is increased slightly for each successive pulse of the source to cover all arrival times. This process can take 1–100 s per scan.

One of the advantages of the conventional time-of-flight mass spectrometer is the opportunity to detect all the ions

from each pulse of the ion source, not just those of a particular mass. In the past this was possible only with an oscilloscope and measurements could only be made directly from the scope or from a photograph of the image on the scope. As a result, time-slice detection has been the predominant method for obtaining recorded or digitized TOF spectra. However, in using TSD, ions of all arrival times other than those observed in the specified time slice are ignored. The result is equivalent to scanning a mass filter, i.e., while ions of one mass are being measured, ions of all other masses are discarded. It has been recently demonstrated that whole sections of a time-of-flight spectrum can be acquired digitally during a single ion pulse (19–21). Though offering improvements, the transient recorders and similar devices used for these studies utilize only a fraction of the mass range and repetition rate capabilities of time-of-flight instruments. A vast improvement in scan speed, sensitivity, and dynamic range could be realized if all ions at every arrival time in each source pulse were acquired at the maximum pulse rate. (This can be called time-array detection or TAD). For typical values of the accelerating voltage (3.5 kV) and analyzer tube length (1.0 m), all ions from one pulse of the source (1–1000 u) will arrive at the detector in less than 40 μ s. Thus, repetition of the ion pulses at a rate of up to 25 kHz will require a detector system with very rapid data throughout. This would be possible with an integrating transient recorder of advanced design. An instrument which can acquire 25 000 complete spectra per second and record up to 1000 averaged spectra per second is currently being developed in our laboratory (22).

Time-array detection will make possible, in a single scan of the magnet, the detection of ions for all values of B and t , i.e., all the daughters of all parents. The result will be a data matrix from which the gamut of MS/MS spectra can be retrieved. Similar data matrices have been obtained in the B - E plane of a double-focusing mass spectrometer, although in these cases multiple scans were necessary to acquire all the data (23, 24). The ability to extract any desired scan from the data matrix by postanalysis processing frees the analyst from the need to decide beforehand which scans would be most useful for a particular sample. The full data matrix would be obtained with TAD in the same time required by any of the single scans with TSD.

Enhancements in sensitivity will be possible with TAD since all ions, not just a selected few, will be monitored for each pulse of the ion source. Even when high resolution in the arrival time is desired, sensitivity for any given measurement coordinate may be lower, but the total signal will still be acquired for all points and the sensitivity can be retrieved during postexperiment processing. Multiple scans of the magnet could be averaged in order to recover the sensitivity lost due to the duty cycle factor. These improvements in sensitivity, together with the ability to obtain the full MS/MS data field in one scan, provide the investigator with a choice. All MS/MS information could be obtained in a small fraction of the time required for the same acquisition by MIKES or TQMS (but with lower sensitivity), or the complete set of MS/MS spectra could be obtained with averaging in the same time as required by MIKES or TQMS (but with higher sensitivity).

The consequence of rapid acquisition of the data matrix will be to open up new opportunities for the full use of MS/MS. The use of a tandem mass spectrometer as a very selective and informative detector for gas and liquid chromatography has in the past been restricted to selected reaction monitoring and very limited scanning of parent or daughter ions. A more rapid acquisition of MS/MS data can make GC/MS/MS and LC/MS/MS much more powerful analytical techniques. Other applications of MS/MS not utilizing on-line

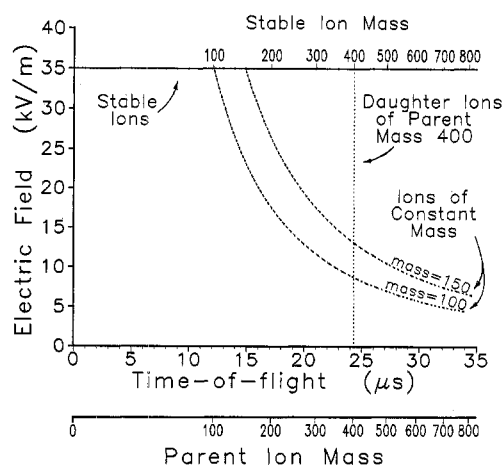


Figure 5. MS/MS data field (E vs. t) for the time-resolved ion kinetic energy spectrometer ($V = 3500$ V, $l = 1.0$ m, $r = 0.2$ m). As in Figure 2, each line represents the locus of peaks for a particular type of ion.

chromatographic separation, such as structure elucidation and studies of fragmentation pathways, could be carried out significantly more rapidly and consequently with much less sample.

Alternative Modes of Operation of the Time-Resolved Magnetic Dispersion Mass Spectrometer. The magnetic field and ion flight time are only two of the three parameters that can be experimentally changed in seeking MS/MS information. According to eq 3 and 5, the accelerating voltage can also be varied. For example, if a constant magnetic field were used, the daughter ion mass would be linearly proportional to the arrival time and the parent ion mass would be obtained from the product Vt^2 . A parent ion scan (constant daughter) could be obtained with TSD by setting t to give a constant value of Bt and scanning V to select different parent ions. However, there are several disadvantages found in scanning and accelerating voltage. These include, (a) loss of sensitivity resulting from defocusing the ion source (25), (b) changes in detector response with different ion energies (26), (c) changes in collision cross-sections with different energies (27), and (d) changes in the relative contribution of thermal energy to the total ion energy.

Ions can also be accelerated to constant momentum, rather than constant energy, by terminating the extraction voltage pulse before any ions can traverse the full field (28). This has the advantage of producing a time-of-flight axis that is linearly related to the parent ion mass.

Implementation of Time Resolution with Other Devices. The concept of time-resolved detection can be employed with other mass spectrometers as well as the magnetic sector mass spectrometer. For example, the electric sector, most often used in double-focusing mass spectrometers and ion kinetic energy spectrometers, is amenable to time-resolved detection (29, 30). The electric sector is an energy filter that obeys eq 10, where E is the electric field at radius r . Ions

$$mv^2/r = zeE \quad (10)$$

are accelerated to constant energy in the source and normally the electric field is adjusted to pass ions of that energy. Excepting any postacceleration decomposition, time-resolved detection of the ions would be equivalent to time-of-flight analysis with increased resolution due to energy filtering, with the ion mass being given by eq 3. Were an ion to decompose in the field-free region between the entrance slit and the electric sector, measurement of the ion velocity by its time of flight, eq 3 will yield the parent ion mass as previously shown, independent of the ion momentum. Measurement of both ion velocity and electric field strength will yield the

daughter ion mass, eq 11. Equation 11 follows from eq 10

$$\frac{m}{z} = \frac{e r E t^2}{l^2} \quad (11)$$

by replacing the velocity with the flight time. Figure 5, analogous to Figure 2, shows the relationship to electric field and arrival time for differential types of ions in the time-resolved ion kinetic energy spectrometer.

Various combinations of mass dispersive fields, such as found in double-focusing instruments, could also utilize time-resolved detection. For a normal geometry double-focusing mass spectrometer, decompositions in the first field-free region would then be energy filtered before time-resolved magnetic dispersion mass spectrometry. Decomposition in the second field-free region would give energy filtered parent ions prior to decomposition. The magnetic sector would momentum-select the stable ions and the daughters produced in the second field-free region. For a reversed geometry instrument, decompositions in the first field-free region would be momentum filtered prior to time-resolved ion kinetic energy spectrometry. Decomposition in the second field-free region would allow the operator to select parent ions both by momentum and time-of-flight thus eliminating the possible ambiguity in parent ion mass assignment found with conventional time-resolved magnetic dispersion mass spectrometry. If decompositions occur in both field-free regions, daughter ions formed in the first field-free region can undergo subsequent fragmentation to form granddaughter ions, both of which can be measured for an additional dimension of information.

CONCLUSION

The time-resolved magnetic dispersion mass spectrometer offers a new and potentially advantageous form of MS/MS. Existing single sector mass spectrometers could be modified for time-resolved detection, thus inexpensively extending the capabilities for MS/MS to many laboratories already equipped with magnetic sector spectrometers. The addition of an integrating transient recorder to this instrument would increase the data throughput significantly. Once sufficient sensitivity is realized, the capabilities for performing GC/MS/MS or LC/MS/MS (to obtain all available MS/MS data on each chromatographic peak) could provide significant improvements in the speed and selectivity of analysis.

ACKNOWLEDGMENT

The authors gratefully acknowledge J. Throck Watson, John Allison, J. David Pinkston, Bruce Newcome, and Brian D. Musselman for many creative discussions which led to the present understanding of the technique.

LITERATURE CITED

- (1) McLafferty, F. W. *Acc. Chem. Res.* **1980**, *13*, 33-39.
- (2) McLafferty, F. W. *Science* **1981**, *214*, 280-287.
- (3) Cooks, R. G.; Glush, G. L. *Chem. Eng. News* **1981**, *59* (48), 40-52.
- (4) Beynon, J. H.; Cooks, R. G.; Amy, J. W.; Baitinger, W. E.; Ridley, T. Y. *Anal. Chem.* **1973**, *45*, 1023A-1031A.
- (5) Yost, R. A.; Enke, C. G. *Anal. Chem.* **1979**, *51*, 1251A-1264A.
- (6) Cooks, R. G.; Beynon, J. H.; Caprioli, R. M.; Lester, G. R. "Metastable Ions"; Elsevier: New York, 1973; pp 59-60.
- (7) Bakker, J. M. B. *J. Phys. E* **1973**, *6*, 785-789.
- (8) Bakker, J. M. B. *J. Phys. E* **1974**, *7*, 364-368.
- (9) Wachs, T.; Bente, P. F.; McLafferty, F. W. *Int. J. Mass Spectrom. Ion Phys.* **1972**, *9*, 333-341.
- (10) Hwang, C.; Kliser, R. W. *Int. J. Mass Spectrom. Ion Phys.* **1978**, *27*, 209-226.
- (11) Holmes, J. L.; Terlouw, J. K. *Org. Mass Spectrom.* **1980**, *15*, 383-396.
- (12) Wiley, W. C.; McLaren, I. H. *Rev. Sci. Instrum.* **1955**, *26*, 1150-1157.
- (13) Sanzone, G. *Rev. Sci. Instrum.* **1970**, *41*, 741-742.
- (14) Stein, R. *Int. J. Mass. Spectrom. Ion Phys.* **1974**, *14*, 205-218.
- (15) Bykovskii, Yu. A.; Dorofeev, V. I.; Dymovich, V. I.; Nikolaev, B. I.; Ryzhikh, S. V.; Silnov, S. M. *Sov. Phys.—Tech. Phys. (Engl. Transl.)* **1969**, *13*, 986-988; *Zh. Tekh. Fiz.* **1968**, *38*, 1194-1196.
- (16) Kovalev, N. D.; Shmikk, D. V.; Feoktistov, I. Yu. *Sov. Phys.—Tech. Phys. (Engl. Transl.)* **1978**, *23*, 718-720; *Zh. Tekh. Fiz.* **1978**, *48*, 1282-1285.
- (17) Poschenrieder, W. P. *Int. J. Mass Spectrom. Ion Phys.* **1971**, *6*, 413-426.
- (18) Mamyrin, B. A.; Karatev, V. I.; Shmikk, D. V.; Zagulin, V. A. *Sov. Phys.—JETP (Engl. Transl.)* **1973**, *37*, 45-48; *Zh. Eksp. Teor. Fiz.* **1973**, *64*, 82-89.
- (19) Dunbar, R. C.; Armentrout, P. *Int. J. Mass Spectrom. Ion Phys.* **1977**, *24*, 465-468.
- (20) Lincoln, K. A. *Dyn. Mass Spectrom.* **1981**, *6*, 111-119.
- (21) Denoyer, E.; Van Grieken, R.; Adams, F.; Natusch, D. F. S. *Anal. Chem.* **1982**, *54*, 26A-41A.
- (22) Holland, J. F.; Enke, C. G.; Watson, J. T.; Allison, J.; Pinkston, J. D.; Stults, J. T.; Newcome, B., manuscript in preparation.
- (23) Coutant, J. E.; McLafferty, F. W. *Int. J. Mass Spectrom. Ion Phys.* **1972**, *8*, 323-339.
- (24) Warburton, G. A.; Stradling, R. S.; Mason, P. S.; Farncombe, M. *Org. Mass Spectrom.* **1981**, *16*, 507-511.
- (25) Sweeley, C. C.; Holland, J. F.; Young, N. D.; Blaiser, R. B. Presented at the 22nd Annual Conference on Mass Spectrometry and Allied Topics, Philadelphia, PA, May 19-24, 1974.
- (26) LaLau, C. In "Advances in Analytical Chemistry and Instrumentation"; Burlingame, A. L., Ed.; Wiley-Interscience: New York, 1970; Vol. 8, pp 93-120.
- (27) Yamaoka, H.; Dong, P.; Durup, J. J. *Chem. Phys.* **1969**, *51*, 3465-3476.
- (28) Wolff, M. M.; Stephens, W. E. *Rev. Sci. Instrum.* **1953**, *24*, 616-617.
- (29) Eubank, H. P.; Wilkerson, T. D. *Rev. Sci. Instrum.* **1963**, *34*, 12-18.
- (30) Warmack, R. J.; Stockdale, J. A. D.; Compton, R. N. *Int. J. Mass Spectrom. Ion Phys.* **1978**, *27*, 239-247.

RECEIVED for review August 3, 1982. Resubmitted March 21, 1983. Accepted March 21, 1983. This work was supported in part by the National Institutes of Health (RR 00480 and GM 28254) and the Office of Naval Research. Portions of this work were presented at the 30th Annual Conference on Mass Spectrometry and Allied Topics, Honolulu, HI, 1982, and the 9th International Mass Spectrometry Conference, Vienna, Austria, 1982.